



Universiteit  
Leiden  
The Netherlands

## **Molecular pathology of hereditary cerebral hemorrhage with amyloidosis-Dutch type**

Grand Moursel, L.

### **Citation**

Grand Moursel, L. (2019, November 21). *Molecular pathology of hereditary cerebral hemorrhage with amyloidosis-Dutch type*. Retrieved from <https://hdl.handle.net/1887/80759>

Version: Publisher's Version

License: [Licence agreement concerning inclusion of doctoral thesis in the Institutional Repository of the University of Leiden](#)

Downloaded from: <https://hdl.handle.net/1887/80759>

**Note:** To cite this publication please use the final published version (if applicable).

Cover Page



Universiteit Leiden



The handle <http://hdl.handle.net/1887/80759> holds various files of this Leiden University dissertation.

**Author:** Grand Moursel, L.

**Title:** Molecular pathology of hereditary cerebral hemorrhage with amyloidosis-Dutch type

**Issue Date:** 2019-11-21

## Chapter 4

# Cerebral amyloid angiopathy with vascular iron accumulation and calcification: a high-resolution MRI-histopathology study

Marjolein Bulk<sup>1,2</sup>, Laure Grand Moursel<sup>1,2</sup>, Linda M. van der Graaf<sup>1,2</sup>, Susanne J. van Veluw<sup>3</sup>, Steven M. Greenberg<sup>3</sup>, Sjoerd van Duinen<sup>4</sup>, Mark van Buchem<sup>1</sup>, Sanneke van Rooden<sup>1</sup>, Louise van der Weerd<sup>1,2</sup>

<sup>1</sup> Department of Radiology, Leiden University Medical Center

<sup>2</sup> Department of Human Genetics, Leiden University Medical Center

<sup>3</sup> Department of Neurology, Massachusetts General Hospital and Harvard Medical School, Boston

<sup>4</sup> Department of Pathology, Leiden University Medical Center

*Adapted from Stroke (2018).*

## Abstract

**Background and Purpose:** Previous studies of symptomatic and asymptomatic hereditary cerebral amyloid angiopathy (CAA) patients offered the possibility to study the radiologic manifestations of CAA in the early stages of the disease. Recently, a ‘striped cortex’, observable as hypointense lines perpendicular to the pial surface on T2\*-weighted 7T MRI, was detected in 40% of the symptomatic hereditary CAA patients. However, the origin of these MRI contrast changes is unknown. This study aimed at defining the underlying pathology associated with the *in vivo* observed striped pattern.

**Methods:** Formalin-fixed *post mortem* brain material including the occipital lobe of four Hereditary Cerebral Haemorrhage with Amyloidosis-Dutch type (HCHWA-D) cases and six sporadic CAA (sCAA) cases were selected from local neuropathology tissue collections. Depending on the availability of the material, intact hemispheres or brain slabs including the occipital lobe of these patients were screened for the presence of a striped cortex. Regions containing the striped cortex were then subjected to high-resolution 7T MRI and histopathological examination.

**Results:** We found two HCHWA-D cases and one sCAA case with striped patterns in the occipital cortex resembling the *in vivo* signal. Histopathological examination showed that the striped pattern in the cortex at 7T MRI is due to iron accumulation and calcification of penetrating arteries. The presence of both non-heme iron and calcification on penetrating arteries causes signal loss and hence the abnormal striped patterns in the cortical ribbon on T2\*-weighted MRI.

**Conclusion:** We identified iron accumulation and calcification of the vessel wall in HCHWA-D as the histopathological correlates of the striped cortex observed on *in vivo* 7T MRI.

## Introduction

Hereditary Cerebral Haemorrhage with Amyloidosis-Dutch type (HCHWA-D) is a genetic disorder caused by a point mutation in the Amyloid Precursor Protein (APP; p.Glu693Gln mutation), resulting in severe cerebral amyloid angiopathy (CAA) characterized by recurrent haemorrhagic strokes with midlife onset (1, 2). Since sporadic CAA (sCAA) is also a disease of the elderly and a common feature in Alzheimer’s disease, the diagnostic point mutation makes HCHWA-D a useful model to study CAA *in vivo* (2).

Previous studies of symptomatic and asymptomatic HCHWA-D mutation carriers offered the possibility to study the radiologic manifestations of CAA pathology during the course of the disease. A ‘striped cortex’, observable as hypointense lines perpendicular to the pial surface on T<sub>2</sub>\*-weighted 7T MRI, was detected in 40% of the symptomatic mutation carriers, specifically in the occipital lobe (3). This pattern was only seen in advanced disease stages and not in asymptomatic patients. However, the underlying pathology of this pattern is unknown.

The feasibility of investigating histopathological correlates of MRI abnormalities have been previously shown in *post mortem* brain tissue (4-6). In the context of CAA, high-resolution *ex vivo* 7T MRI scanning allowed the detection of microvascular lesions, including microhaemorrhages, microinfarcts, and CAA-related vasculopathies (6).

The aim of this study was to define the underlying pathology associated with the *in vivo* observed striped pattern. Therefore, we screened *post mortem* brain material of four HCHWA-D donors from our local neuropathology tissue collection using 7T MRI. In two cases, striped patterns in the occipital cortex resembling the *in vivo* signal were detected. These areas were subjected to high-resolution 7T MRI to study the pattern in greater detail. Based on our hypothesis that the observed MRI contrast might be due to calcification, we added a micro computed tomography (μCT) scan as this modality is the most sensitive and specific imaging tool allowing for the identification of calcifications (7). Serial sections of the identified areas were further subjected to histological investigation to examine the histopathological correlates of the distinctive striped MRI pattern. Since HCHWA-D serves as a model for sCAA, we additionally retrospectively screened previously acquired whole hemisphere *ex vivo* 3T MRI scans of six sCAA cases. In one case (with severe CAA) a striped pattern was observed in the occipital cortex. Brain samples from that area were then subjected to 7T MRI and subsequent histopathological examination.

## Material and Methods

The data that support the findings of this study are available from the corresponding author upon reasonable request.

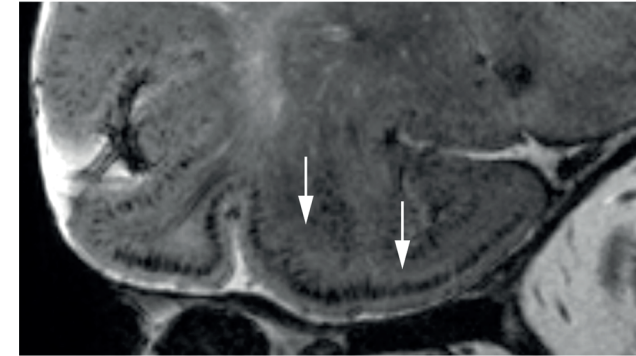
### Study design

Formalin-fixed *post mortem* brain material including the occipital lobe of four HCHWA-D cases were selected from the neuropathology tissue collection of the Leiden University Medical Center (LUMC) in Leiden (The Netherlands) (see workflow in Fig. 1). Depending on the availability of the material, intact hemispheres or brain slabs including the occipital lobe of these patients were scanned at 7T MRI. The 7T MR images were visually inspected by two experienced observers (SvR, LvdW) and screened for a striped cortical pattern defined as hypointense lines perpendicular to the pial surface (3). Two cases showed a striped cortex on 7T MR images and smaller tissue blocks from these cases were further investigated on high-resolution 7T MRI and histology. Based on our hypothesis that the observed MRI contrast might be due to calcification, we added an  $\mu$ CT scan as this modality is the most sensitive and specific imaging tool allowing for the identification of calcifications (7). In addition, *ex vivo* 3T MRI scans from six sCAA cases, acquired at the Massachusetts General Hospital (MGH) in Boston (MA, USA) were retrospectively screened for the presence of a striped cortex. This pattern was observed in one sCAA case, which was then subjected to 7T MRI and histopathological examination. Case characteristics of screened HCHWA-D and sCAA cases are presented in Table 1.

**Table 1:** Characteristics of screened HCHWA-D and sCAA cases.

	Age	Sex	<i>Post mortem</i> delay (hours)	Striped cortex detected
HCHWA-D #1	70	Female	5	Yes
HCHWA-D #2	57	Male	2,5	Yes
HCHWA-D #3	50	Female	16	No
HCHWA-D #4	50	Male	19	No
sCAA #1	70	Male	16	Yes
sCAA #2	80	Male	Unknown	No
sCAA #3	76	Male	27	No
sCAA #4	65	Male	14	No
sCAA #5	81	Male	Unknown	No
sCAA #6	70	Female	Unknown	No

### Striped cortex in vivo in symptomatic HCHWA-D patients observed at 7T MRI<sup>3</sup>



#### Step 1: Detection of the striped cortex on *ex vivo* MRI

*Post mortem* formalin-fixed hemispheres/brain slabs of HCHWA-D (n=4) cases stored in the local neuropathology tissue collection were scanned and screened

#### Step 2: High-resolution 7T MRI and $\mu$ CT of positive cases (HCHWA-D 2 cases, sCAA 1 case)

A small tissue block corresponding to a striped pattern area was resected and imaged with high resolution 7T MRI and CT

#### Step 3: Investigation of the histopathological correlates of the cortical changes detected at 7T MRI

Tissue blocks from step 2 were paraffin embedded. Tissue sectioning was guided by the *post mortem* MRI and based on anatomical landmarks such as the grey-white matter border, vessels, and the orientation of the striped pattern.

Histopathological assessment included staining for: iron, calcification, A $\beta$ , H&E

**Figure 1:** Study design and flowchart.

### Brain samples and preparation

Formalin-fixed intact hemispheres or brain slabs of HCHWA-D patients were obtained from the local neuropathology tissue collection of the LUMC. Written informed consent for the HCHWA-D patients was obtained for each donor and all material and data were handled in a coded fashion maintaining patient anonymity according to Dutch national ethical guidelines (Code for Proper Secondary Use of Human Tissue, Dutch Federation of Medical Scientific Societies). Formalin-fixed intact hemispheres of the sCAA cases were obtained through an ongoing *post mortem* brain MRI study for the evaluation of MRI markers in the context of sporadic CAA at the MGH in Boston (MA, USA). Informed consent was obtained from a legal

representative prior to brain autopsy. This study was approved by the local Ethics Committees of the respective institutions.

Before MRI, the formalin-fixed brain material of the HCHWA-D patients was washed with phosphate buffered saline (PBS) for 24 h to partially restore the relaxation parameters (8). The hemisphere or brain slabs were placed in a plastic bag containing a proton-free fluid (Fomblin®, LC08, Solvay). To minimize the amount of trapped air bubbles, a vacuum was applied overnight. Before scanning, the plastic bag was sealed and fixed on a plastic plateau or using foam padding in the coil.

After scanning the intact hemisphere and brain slabs, the scans were inspected for the presence of a striped cortex by two experienced observers (SvR, LvdW). If positive, a small tissue block of approximately 20x15x15 mm was resected from the area containing the striped cortex and placed in a regular 15 ml tube (Greiner Bio-One). Before MRI, the tissue block was washed with PBS (for 24 h) to partially restore the relaxation parameters (8). Next, the 15 ml tube containing the tissue block was filled with Fomblin® (LC08, Solvay). Care was taken to avoid trapped air bubbles.

### ***Post mortem MRI acquisition***

The HCHWA-D hemispheres were scanned at the LUMC (Leiden, the Netherlands) on a whole-body human 7T MR system (Philips Healthcare, Best, the Netherlands) using a quadrature transmit and 32-channel receiver head coil. The hemisphere was positioned with the frontal lobe in the head direction and the occipital lobe in the feet direction of the scanner. A 2D  $T_2^*$ -weighted gradient echo scan was acquired with a total imaging duration of 13 minutes. Imaging parameters were: repetition time (TR)/echo time (TE) 3146/25 ms, flip angle 60°, slice thickness 1.0 mm with a 1.1 mm interslice gap and a spatial resolution of 0.21x0.21 mm.

The HCHWA-D brain slabs and smaller tissue blocks were also scanned at the LUMC (Leiden, the Netherlands), but on a 7T horizontal bore Bruker MRI system equipped with a 23 mm receiver coil (Bruker Biospin, Ettlingen, Germany). The smaller tissue blocks were scanned with a Multiple Gradient Echo (MGE) sequence using the following parameters: (TR)/(TE) 75/12.5, 23.2, 33.9 and 44.6 ms, flip angle 25°, at 100  $\mu$ m isotropic resolution with 20 signal averages.

Brain slabs of one sCAA case that demonstrated a striped pattern on previously acquired whole hemisphere *ex vivo* 3T MRI scans, were subsequently scanned at 7T MRI. Scanning was performed at the Athinoula A. Martinos Center for Biomedical Imaging (MGH, Charlestown, MA, USA), on a whole-body human 7T MR Siemens MAGNETOM scanner, using a custom built 32-channel head coil, as described previously (6).

Slabs were stacked on top of each other in a glass beaker, filled with 10% formalin. A multi-echo  $T_2^*$ -weighted MRI scan was acquired using the following parameters: one run each of three flip angles (10°, 20°, and 30°), TE = 8, 18, 28, and 38 ms, at 200  $\mu$ m isotropic resolution.

The most similar MRI slice with respect to the given histology was selected based on the physical location of the section in the tissue block, measured by counting the number of sections taken starting at the block surface. At this approximate location, the most similar MRI slice was chosen by visual comparing clearly detectable landmarks (contours, vasculature, tears etc.) allowing comparison of the MRI with histology.

### ***Post mortem $\mu$ CT***

For the HCHWA-D cases, MRI acquisition was followed by  $\mu$ CT to detect the presence of calcifications. The 15 ml tube containing the tissue block in Fomblin was imaged on a Skyscan 1076 *in vivo*  $\mu$ CT (Bruker Biospin, Ettlingen, Germany) using the following settings: 40-48 kV, 200-250  $\mu$ A, 0.5 mm filter, 2-10 averages. The same approach as described above for the MRI slice selection was used to select the most similar  $\mu$ CT image.

### ***Histology and immunohistochemistry***

The resected tissue blocks used for both MRI and  $\mu$ CT were next subjected to detailed histopathologic examination. Each tissue block was embedded in paraffin, and subsequently cut in 5  $\mu$ m-thick serial sections on a microtome. The sectioning was guided by the *post mortem* MRI scans based on anatomical landmarks such as the grey-white matter border, vessels, and the orientation of the striped pattern.

The first section was stained for A $\beta$  (anti-human A $\beta$ , 6F/3D DakoCytomation, Glostrup, Denmark): endogenous peroxidase activity was blocked with 0.3% H<sub>2</sub>O<sub>2</sub> in methanol followed by an antigen retrieval step using formic acid and trypsin. The primary antibody was incubated overnight at room temperature. The secondary antibody was incubated for one hour followed by a 30 minutes incubation with avidin-biotin complex (ABC, Vector Labs, CA, USA). Signal enhancement was completed by immersion in 3,3'-Diaminobenzidine (DAB). Finally, sections were counterstained with Harris Haematoxylin.

Adjacent sections were stained with the Von Kossa technique to detect calcification and a standard hematoxylin & eosin (H&E) staining. For the detection of iron, two protocols were used. For each case one section was stained using the classic Perls' Prussian blue iron stain. In addition, one section was stained according to an in-house protocol of a modified Meguro staining (9). In short, sections were incubated for 30 minutes in 1% potassium ferrocyanide, washed, followed by 60 minutes incubation in

methanol with 0.01 M  $\text{NaN}_3$  and 0.3%  $\text{H}_2\text{O}_2$ . Subsequently, sections were washed with 0.1 M phosphate buffer followed by 30 minutes incubation in a solution containing 0.025% 3'3-DAB-tetrahydrochloride (DakoCytomation) and 0.005%  $\text{H}_2\text{O}_2$  in 0.1 M phosphate buffer. The reaction was stopped by washing in demi water.

Tissue blocks from the sCAA case were processed in a similar fashion. Sections underwent histological staining with H&E, Perls' Prussian blue iron, and Von Kossa, and immunohistochemistry against  $\text{A}\beta$  (6F/3D, Dako).

All slides were digitized using an automatic bright field microscope (Philips Ultra Fast Scanner, Philips, Netherlands) for microscopic evaluation. All stained sections were independently evaluated by LGM, MB and SvV for the amount of  $\text{A}\beta$ , iron and calcium positive vessels. For both HCHWA-D subjects one area with the striped cortex, one area without the striped cortex and one area with some contrast changes were scored. Percentages were calculated for the amount of vessels positive and negative for iron and calcium with respect to the total number of  $\text{A}\beta$  positive vessels.

## Results

### Detection of the striped cortex *ex vivo*

*Post mortem* brain material of four HCHWA-D were scanned at 7T and in two out of four HCHWA-D cases a striped pattern was found *ex vivo* in the occipital cortex, similar to the *in vivo* MRI observation (Fig. 2A). In both HCHWA-D cases, also areas with normal contrast were observed on high-resolution *ex vivo* 7T MRI. In one out of six cases with sCAA screened for this study, a similar striped pattern as in the HCHWA-D cases was observed in the occipital cortex (Fig. 3A).

### $\mu\text{CT}$ and histopathological correlates of the striped cortex

Given the shape and course of the striped cortex, we hypothesised that the observed MRI contrast changes may be caused by  $\text{A}\beta$  depositions in the walls of perforating arteries, co-localizing with iron accumulation and calcifications.

Microscopic examination showed severe and widespread CAA in both HCHWA-D cases (Fig. 2C). The sCAA case was also characterised by severe and widespread CAA and more than 200 microbleeds on *ex vivo* 3T MRI (Fig. 3B). No noticeable differences in vessel wall morphology or  $\text{A}\beta$  staining of angiopathic arterioles was observed between areas with and without the striped cortex. Old microhemorrhages in the form of focal hemosiderin deposits were not evident in the examined tissue sections.

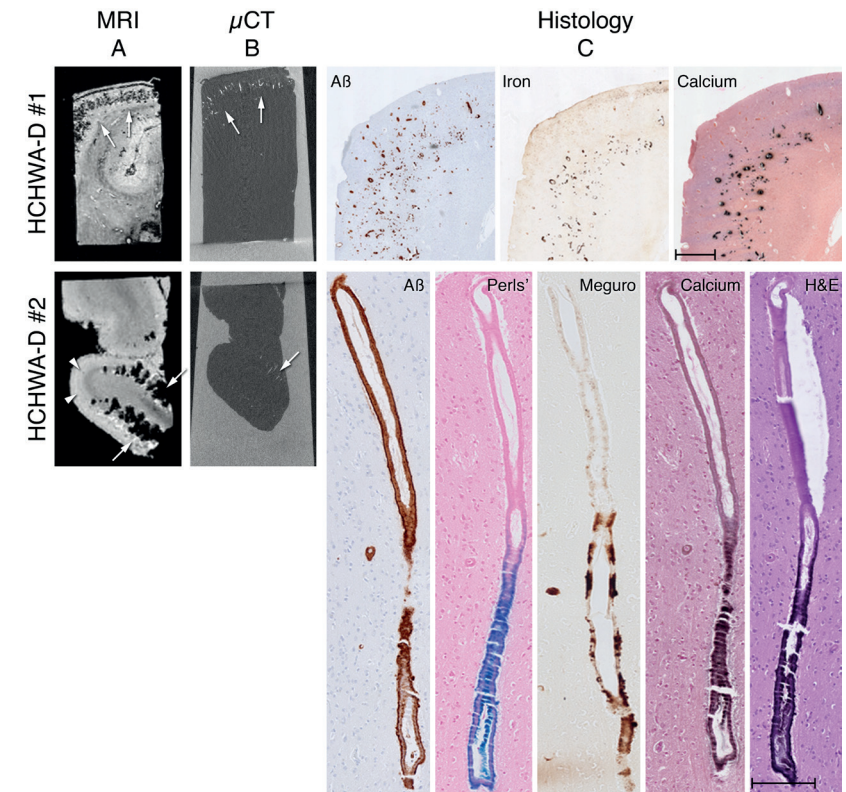


**Figure 2: MRI,  $\mu\text{CT}$  and histology of the striped cortex in HCHWA-D.** A striped pattern resembling the *in vivo* findings was found in the occipital lobe of HCHWA-D patient 1 (A, first row) and HCHWA-D patient 2 (A, second row). High-resolution 7T MRI (TE 12.5 ms) showed a striped pattern of the cortex (arrows) in addition to some parts of the cortical ribbon showing normal cortical contrast (arrowheads). (B) Vascular calcifications were confirmed by  $\mu\text{CT}$  (arrows). (C) Histopathological examination showed that the majority of the cortical vessels stained positive for  $\text{A}\beta$ . Interestingly, only vessels in the middle to deeper cortical layers stained positive for non-heme iron (Meguro) and calcium (Von Kossa), indicating iron accumulation and calcification of the vessel wall in specific cortical layers. In contrast to  $\text{A}\beta$ , which was observed over the full length of the perforating arteries, non-heme iron (Perls' and Meguro) and calcium (Von Kossa) was only observed in the lower part of the vessel. Calcification of the vessel wall was also visible on the H&E staining as deep purple depositions. C first row as well as C second row are consecutive slides. Orientation histology: top = leptomeninges; bottom = white matter. Scale bars in C first row = 1 mm, C second row = 200  $\mu\text{m}$ .

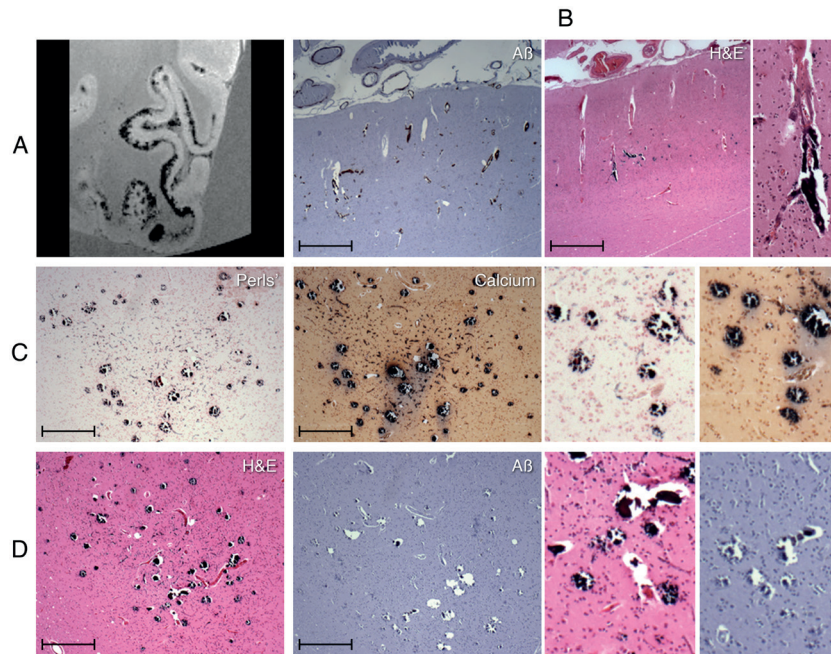


**Figure 3: Striped cortex in a sporadic CAA case.** (A) A similar striped pattern as in the HCHWA-D cases was observed in the occipital cortex of a sporadic CAA case on high-resolution 7T MRI. (B) This case was characterised by severe and widespread CAA and more than 200 microbleeds on ex vivo 3T MRI. (C) Histological examination showed the same co-localization in the vessel wall as observed in the HCHWA-D patients, namely: non-heme iron (Perls') and calcium (Von Kossa). Calcification of the vessel wall was also visible on the H&E staining as deep purple depositions. (D) Interestingly, in contrast with the HCHWA-D cases, iron accumulation and calcification was also observed in vessels without CAA. Scale bars = 500  $\mu$ m.

In both HCHWA-D cases and the sCAA case, co-localization of A $\beta$  with non-heme iron and calcium in the vessel wall was found in areas containing the striped cortex (Fig. 2, 3, Suppl. Fig. I, Suppl. Fig. II, Suppl. Table I). In contrast to A $\beta$ , which was observed over the full length of the perforating arteries, non-heme iron and calcium were only observed in the lower part of the vessel (Fig. 2C). Calcification of the vessel wall was also visible in the H&E staining as deep purple depositions and confirmed by  $\mu$ CT (Fig. 2, 3). Interestingly, in contrast to the HCHWA-D cases, in sCAA, iron accumulation and calcification was also observed in vessels without CAA (Fig. 3D).

In addition, a hypointense line in the superficial cortical layers parallel to the cortical surface was observed in one of the HCHWA-D cases, resembling superficial siderosis. Histology showed co-localization with local iron accumulation in neurons in layer II of the cortex (Suppl. Fig. III).

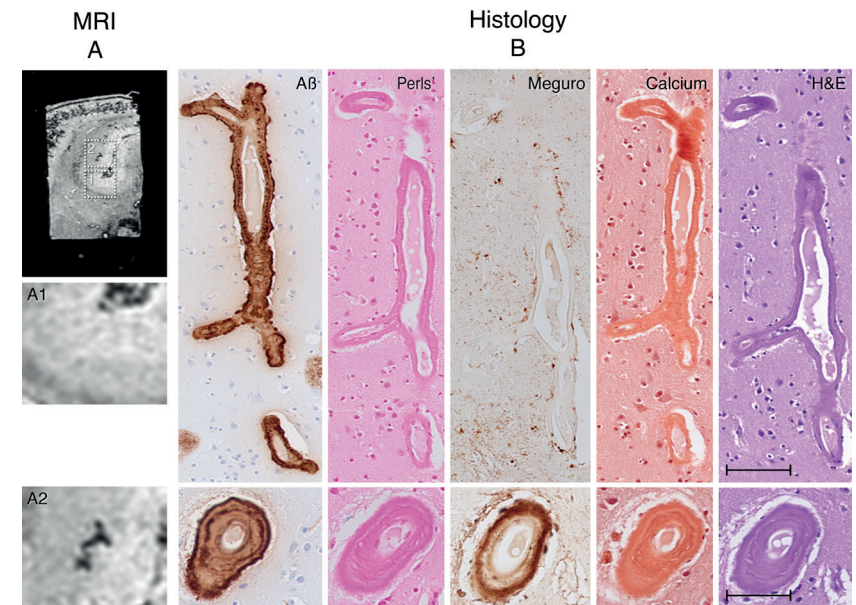


**Figure 4: Zoomed MRI and histology of an area outside the 'striped cortex' in HCHWA-D patient 1.** High-resolution 7T MRI (TE 12.5 ms) and zoom of an area without the striped cortex (A1) and an area with some contrast changes (A2). (B) Histopathological examination showed that most cortical vessels stained positive for A $\beta$  in both areas. However, in areas without the striped cortex vessels were negative for non-heme iron (Perls' and Meguro) and calcium (Von Kossa). Also the H&E staining was negative. In areas with some contrast changes (A2), although less intense, these contrast changes correlated with an area where we found vessels positive for non-heme iron detected by the Meguro staining. The Perls', calcium and H&E stainings were negative. (B) are consecutive slides. Orientation histology: top = leptomeninges; bottom = white matter. Scale bars in B-F = 100  $\mu$ m; G-K = 50  $\mu$ m.

### Histopathological correlate of areas outside the striped cortex

To confirm specificity of iron accumulation and calcification in the vessel wall as the histopathological correlate of the striped cortex, we further investigated other regions of the cortex in HCHWA-D tissue (Fig. 4A).

On histology, most cortical vessels stained positive for A $\beta$ , also in areas without the striped pattern on MRI. However, these vessels were negative for non-heme iron and calcium (Fig. 4B, Suppl. Table I). We also noticed some areas outside the striped cortex with contrast changes on MRI which had a similar pattern, but that were less intense than the striped pattern described above. These MRI contrast changes may be due to vessels positive for A $\beta$  and non-heme iron, but negative for calcium (Fig. 4B, Suppl. Table I). Calcification without iron accumulation was not observed.



## Discussion

Our findings show that the recently observed striped pattern in the cortex of symptomatic HCHWA-D patients at 7T MRI is due to iron accumulation and calcification of A $\beta$  positive penetrating arteries. The presence of both non-heme iron and calcification on penetrating arteries causes signal loss and hence abnormal cortical patterns on T<sub>2</sub>\*-weighted MRI.

As reported, on *in vivo* 7T MRI the striped cortex was found in 40% of the symptomatic HCHWA-D patients. Since the striped cortex was not found in presymptomatic mutation carriers, it might be associated with more advanced stages of the disease (3). Typically, the first stroke occurs between the ages of 39 and 76 years (mean 50 years) and is fatal for one-third of the patients. Those who survive suffer from recurrent strokes resulting in severe disabilities. In exceptional cases, people survive longer, with a maximum reported survival of 28 years (10). Histopathological examination showed that both the HCHWA-D cases and the sCAA case were characterized by a severe and widespread CAA. This suggests that the striped cortex may be a marker of advanced CAA.

Mineral substances such as iron and calcium are known as paramagnetic materials and have consistently been reported to cause hypointense signals on T<sub>2</sub>\*-weighted MRI images (5, 11). It is known that in patients with Alzheimer's disease and concomitant severe CAA have higher non-heme iron content in the temporal lobe than Alzheimer patients without CAA and that divalent iron accumulates within CAA-positive vessel walls (12). Iron-positive CAA vessels have also been reported in HCHWA-D patients (13, 14). Moreover, some of the largest cortical CAA vessels positive for iron were observed on histology and could be topographically matched with *ex vivo* high-resolution 9.4T MRI (13). Corresponding to our results, Nabuurs et al. showed that not all CAA-affected vessels resulted in a similar loss of MR signal (13). These different effects on MRI were thought to be caused by differences in the amount of A $\beta$ , its positioning in the vessel wall or other associated microvasculopathies. Here we showed that A $\beta$  depositions in and along the penetrating vessels are not in itself resulting in T<sub>2</sub>\*-weighted MRI contrast; CAA vessels without iron accumulation and calcification resulted in normal MRI signal, whereas the presence of iron alone or both iron and calcium resulted in the detection of hypointense signals on T<sub>2</sub>\*-weighted MRI.

These iron-sensitive MRI scans have been previously used to detect for example superficial siderosis, large intracerebral haemorrhage and (cortical) microbleeds. MRI-observed microbleeds, visible as small round hypointense lesions on T<sub>2</sub>\*-weighted MRI, correlate to acute microhaemorrhages or iron-positive old microhaemorrhages on histopathology (6). Of note, in our cases the observed striped cortex was not associated with acute or old haemorrhages on histopathology.

Apart from iron accumulation in CAA vessels, we also observed calcification of the vessel wall. Calcification of CAA vessels has been previously reported in very severe CAA cases; cortical calcifications were found using histopathology in p.Glu692 Gln (Dutch) patients (15) and using CT in patients with p.Glu693Lys (Italian) and p.Asp694Asn (Iowa) mutations (16). However, iron accumulation and calcifications as detected by 7T MRI in patients with the p.Glu693Gln mutation (Dutch) have not been reported previously and the underlying mechanisms of vascular iron accumulation and calcifications in APP mutation carriers are unknown. The striped cortex was found in the occipital cortex on *in vivo* MRI (3), which seems to be consistent with the posterior predominance of CAA severity. In addition, we showed that predominantly vessels in the middle cortical layers accumulated iron and calcium. Why specific regions and cortical layers are more affected than others remains to be elucidated. Lastly, we showed that some vessels only accumulated iron but no calcification, whereas we did not find any vessels with calcifications without iron. Based on these observations we speculate that in HCHWA-D A $\beta$  depositions in the vessel wall are followed by iron accumulation, resulting eventually in calcifications of the vessel wall.

## Conclusions

In conclusion, we identified iron accumulation and calcification of the vessel wall in HCHWA-D as the histopathological correlates of the striped cortex observed on *in vivo* 7T MRI. This novel MRI marker is of interest for clinical CAA severity evaluation as it was also observed in a case with severe sCAA. Associated mechanisms resulting in iron accumulation and calcification of CAA vessels will need further investigation.

## Acknowledgement

The authors thank I. M. Hegeman-Kleinn for her technical assistance and Ernst Suidgeest for 7T MRI acquisition of the HCHWA-D brain slabs.

## Sources of funding

SJvV receives funding from the Netherlands Organisation for Scientific Research (Rubicon fellowship grant # 019.153LW.014).

## Disclosures

None

## Supplementary Material

The Supplementary Material for this article can be found online at:

<https://www.ahajournals.org/doi/suppl/10.1161/STROKEAHA.118.021872>

## References

1. Kamp JA, Moursel LG, Haan J, Terwindt GM, Lesnik Oberstein SA, van Duinen SG, et al. Amyloid beta in hereditary cerebral hemorrhage with amyloidosis-dutch type. *Rev Neurosci*. 2014;25:641-651
2. Luyendijk W, Bots GT, Vegter-van der Vlis M, Went LN, Frangione B. Hereditary cerebral haemorrhage caused by cortical amyloid angiopathy. *J Neurol Sci*. 1988;85:267-280
3. Koemans EA, van Etten ES, van Opstal AM, Labadie G, Terwindt GM, Wermer MJH, et al. Innovative mri markers of hereditary cerebral amyloid angiopathy at 7 tesla. *Stroke*. 2018;In press
4. Bulk M, Abdelmoula WM, Nabuurs RJA, van der Graaf LM, Mulders CWH, Mulder AA, et al. Postmortem mri and histology demonstrate differential iron accumulation and cortical myelin organization in early- and late-onset alzheimer's disease. *Neurobiol Aging*. 2017;62:231-242
5. Fukunaga M, Li TQ, van Gelderen P, de Zwart JA, Shmueli K, Yao B, et al. Layer-specific variation of iron content in cerebral cortex as a source of mri contrast. *Proc Natl Acad Sci U S A*. 2010;107:3834-3839
6. van Veluw SJ, Charidimou A, van der Kouwe AJ, Lauer A, Reijmer YD, Costantino I, et al. Microbleed and microinfarct detection in amyloid angiopathy: A high-resolution mri-histopathology study. *Brain*. 2016;139:3151-3162
7. Thompson BH, Stanford W. Imaging of coronary calcification by computed tomography. *J Magn Reson Imaging*. 2004;19:720-733
8. Shepherd TM, Thelwall PE, Stanisz GJ, Blackband SJ. Aldehyde fixative solutions alter the water relaxation and diffusion properties of nervous tissue. *Magn Reson Med*. 2009;62:26-34
9. van Duijn S, Nabuurs RJ, van Duinen SG, Natte R. Comparison of histological techniques to visualize iron in paraffin-embedded brain tissue of patients with alzheimer's disease. *J Histochem Cytochem*. 2013;61:785-792
10. Maat-Schieman M, Roos R, van Duinen S. Hereditary cerebral hemorrhage with amyloidosis-dutch type. *Neuropathology*. 2005;25:288-297
11. Langkammer C, Krebs N, Goessler W, Scheurer E, Ebner F, Yen K, et al. Quantitative mr imaging of brain iron: A postmortem validation study. *Radiology*. 2010;257:455-462
12. Schrag M, Crofton A, Zabel M, Jiffry A, Kirsch D, Dickson A, et al. Effect of cerebral amyloid angiopathy on brain iron, copper, and zinc in alzheimer's disease. *J Alzheimers Dis*. 2011;24:137-149
13. Nabuurs RJ, Natte R, de Ronde FM, Hegeman-Kleinn I, Dijkstra J, van Duinen SG, et al. Mr microscopy of human amyloid-beta deposits: Characterization of parenchymal amyloid, diffuse plaques, and vascular amyloid. *J Alzheimers Dis*. 2013;34:1037-1049
14. van Rooden S, Maat-Schieman ML, Nabuurs RJ, van der Weerd L, van Duijn S, van Duinen SG, et al. Cerebral amyloidosis: Postmortem detection with human 7.0-t mr imaging system. *Radiology*. 2009;253:788-796
15. Vinters HV, Natte R, Maat-Schieman ML, van Duinen SG, Hegeman-Kleinn I, Welling-Graafland C, et al. Secondary microvascular degeneration in amyloid angiopathy of patients with hereditary cerebral hemorrhage with amyloidosis, dutch type (hchwa-d). *Acta Neuropathol*. 1998;95:235-244
16. Sellal F, Wallon D, Martinez-Almoyna L, Marelli C, Dhar A, Oesterle H, et al. App mutations in cerebral amyloid angiopathy with or without cortical calcifications: Report of three families and a literature review. *J Alzheimers Dis*. 2017;56:37-46